Submitted to **Journal of the European Optical Society-Rapid Publications**
Template provided by EDP Sciences

Review paper

Integrating Hollow-Core Fibers into Conventional Networks: Coupling Approaches and Performance Evaluation

Muhammad Hanif Ahmed Khan Khushik[1,2*], Shahzadi Bano[3], Luo Yinsheng[1], Lu Sun[4], Guoping Chen[5], Jamal N.A. Hassan[1], Muhammad Saleem[2], Mian Muhammad Kamal[1], Hamedalneel B A Hamid[1], Tianjun Ma [1,*]

[1] School of Electronic and Communication Engineering, Quanzhou University of Information Engineering, Quanzhou 362000, China.
[2] Department of Electronics Engineering Technology, Benazir Bhutto Shaheed University of Technology and Skill Development, Khairpur Mirs 66020, Sindh, Pakistan.
[3] School of Computer and Artificial Intelligence, Zhengzhou University, Zhengzhou 450001, China.
[4] State Key Lab of Photonics and Communications, Department of Electronic Engineering, Shanghai Jiao Tong University, Shanghai 200240, China
[5] School of Information Engineering, Xuzhou University of Technology, Xuzhou, 221018, China.

Abstract – To exploit the performance potential of hollow-core fibers (HCFs) in next-generation photonic systems, their reliable optical interconnection with existing solid-core single-mode fiber (SMF) infrastructure is critical. This review article presents a systematic comparison of the major coupling techniques addressing the solid-core-to-hollow-core transition challenge, including fiber tapering, adhesive bonding, lens-assisted coupling, direct fusion splicing, and connectorized assemblies. Critical performance indicators, such as insertion loss, reflection suppression, modal stability, and thermal stability, are compared across these methods. The comparison shows that the best performance is often fiber-class-dependent (e.g., adhesive bonding yields record-low loss with nested anti-resonant nodeless fibers (NANF) and double-nested anti-resonant nodeless fibers (DNANF), and other HCF classes may be better served by tapering or lens-based coupling methods). This review also considers practical implementation factors, including scalability, yield, and field deployability, and evaluates the relevance of these techniques for 6G transport, quantum links, and high-power photonics applications. By integrating design principles, experimental results, and practical limitations, this article provides a decision-making guide for engineers and identifies key innovation priorities for the seamless integration of HCFs into emerging optical networks.
Keywords: fiber-to-fiber coupling; hollow-core fiber interconnects; mode-field adaptation; waveguide mismatch mitigation

1. Introduction

The dramatic increase in worldwide data rates has revealed the inherent physical constraints of traditional solid-core SMF [1, 2]. Despite their ultralow attenuation (~0.15 dB/km) and well-established manufacturing ecosystem, SMF have a limited performance due to intrinsic constraints. They are nonlinear effects (Kerr nonlinearity and stimulated Raman scattering), Shannon capacity limit, and group velocity dispersion, which limit increased improvements in data rates and signal integrity [3, 4]. An alternative that represents a paradigm shift is hollow-core fibers (HCFs). They use these to trap the majority of optical power in air by manipulating light through an air-filled core [5]. This essentially decreases nonlinear interactions, decreases latency (taking advantage of the increased velocity of light in air), and raises power-handling thresholds[1].

*Muhammad Hanif Ahmed Khan Khushik: hanif.khushk@bbsutsd.edu.pk
Tianjun Ma: mmmmtj@126.com

This provisional PDF is the accepted version. The article should be cited as: J. Eur. Opt. Society-Rapid Publ., https://doi.org/10.1051/jeos/2026055

This means that HCFs are particularly well-suited to high-power laser delivery, ultra-low-latency data delivery, and nonlinearity-sensitive photonic systems [6-8]. The more recent advances in the anti-resonant (AR-HCF) and photonic bandgap (PBGF) designs have reduced their attenuation to levels competitive with conventional SMFs in important spectral bands, highlighting their readiness to be used next-generation applications [9, 10]. Anti-resonant (AR-HCF) and photonic-bandgap (PBGF) structures have recently been developed to push attenuation to the point of competing with standard SMFs in important spectral bands. The main HCF families are photonic-bandgap fibers (PBGFs), Kagome-lattice, nested anti-resonant nodeless fibers (NANFs), and double-nested (DNANFs) that use different guiding mechanisms to provide different bandwidth, modal, and loss properties (Fig. 1). Recent literature, such as Borzycki et al. [11] and Ferriera et.al.,[12] , discusses comprehensive details of HCF design, fabrication, and performance trade-offs. Even with these developments, interoperability of HCFs with the extensive installed base of SMF infrastructure is a critical choke point. The extreme mode-field diameter mismatch (usually 10 µm versus 25-40 µm), high Fresnel reflections at the silica air interface, and the underinsured excitation of higher-order modes (HOMs) routinely result in interconnection losses of over 3 dB and return losses of less than -14 dB, which is why numerous variations of coupling have been developed to respond, including direct and modified fiber fusion splicing, fiber tapering, lens-based free-space coupling, adhesive bonding to mode-field adapters, bridge splicing, and connectorized assemblies. All the techniques have a trade-off between insertion loss, reflections, modal purity, mechanical strength, thermal stability, scalability, and field deployability. The available literature, however, is mostly limited to single experimental demonstrations lacking a common critical framework to compare techniques across HCF geometries and application conditions. This review fills that gap. We show a systematic, comparative analysis of state-of-the-art SMF-to-HCF coupling methodologies. Section 2 establishes a rigorous multi-dimensional evaluation framework covering optical, mechanical, and system-level metrics. Section 3 surveys each major technique, blending physical principles with the latest experimental results and inherent limitations. Section 4 synthesizes performance hierarchies, maps techniques to key application domains (6G transport, quantum networks, high-power photonics, and precision sensing), and identifies optimal use cases. Finally, Section 5 highlights persistent open challenges and outlines targeted research priorities to accelerate the transition of HCFs from laboratory prototypes to widespread network deployment.

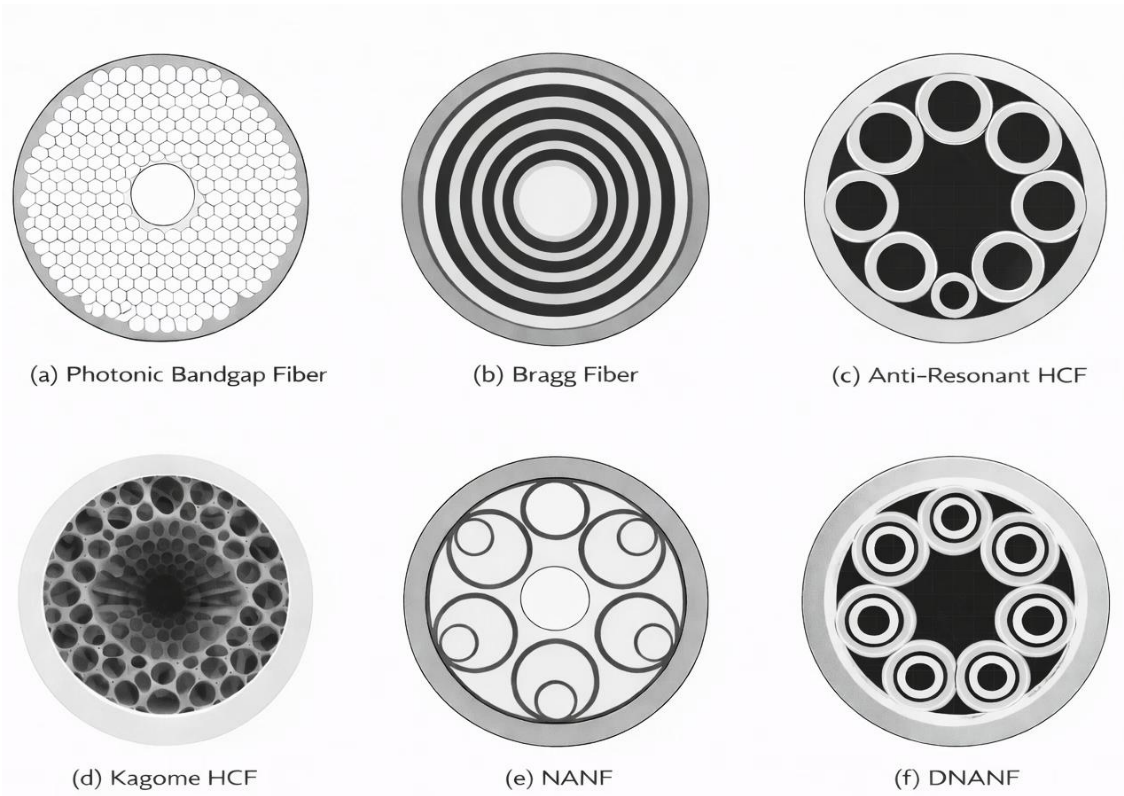

Fig. 1. Schematic diagrams of the various microstructured optical fibers

2. Evaluation Metrics for SMF-HCF Coupling

A coupling technique providing minimum loss, can still be not suitable for a particular application because of higher back-reflection, low durability, high-cost, and complexity in deployment. In this section a review on optical metrics used to compare interconnection techniques, environmental and thermomechanical stability, practical metrics for deployment and scale-up, and system-level relevance of the reported metrics.

2.1 Optical Metrics used to compare interconnection techniques

2.1.1 Mode field Matching and Intrinsic coupling Efficiency

Most studies consider mode-field matching as the vital metric for an SMF–HCF interface. The key parameter is the power coupling efficiency, η_c, which is the measurement of the fraction of input optical power coupled into the desired guided mode of the HCF under ideal conditions, i.e., without considering fabrication defects, environmental perturbations, and parasitic reflections [13, 14]. Here $\eta_{c,}$ does not measure performance of an interconnection, but the intrinsic overlap limit executed due to field distributions of the two waveguides.

Mathematically, η_c can be calculated as the normalized overlap integral between the incident field and the target receiving mode [13, 14]:

$$\eta_c = \frac{\left| \iint_{\infty} E_{SMF}(x,y).E^*_{HCF}(\mathrm{x},\mathrm{y})dxdy \right|^2}{\left(\iint_{\infty} \left|E_{SMF}(x,y)\right|^2 dxdy\right)\left(\iint_{\infty} \left|E_{HCF}(x,y)\right|^2 dxdy\right)} \qquad (1)$$

The associated intrinsic coupling loss is

$$L_{overlap} = -\log_{10}(\eta_{\mathrm{c}}) \qquad (2)$$

η_c is the baseline to compare all the practical interconnection techniques. If measured experimental insertion loss is considerably greater than $L_{overlap}$,the additional loss mostly originates from Fresnel reflections, alignment error, structural deformation happened while processing, or higher-order mode (HOM) excitation. For photonic bandgap and anti-resonant HCFs, the guided mode mostly behaves like non-Gaussian, therefore accurate assessment of η_c relies on numerical mode solving rather than Gaussian approximation [13, 14].

2.1.2 Insertion loss, return loss, and Fresnel Reflection

Insertion loss, and return loss are two most widely used metrics, to judge the applicability of the interconnection technique discussed in section 3.

Insertion loss (IL) is defined as the loss of optical power because of interconnection into an optical path. It is measured in decibels (dB) and mathematically can be given as

$$IL = -10\log_{10}\left(\frac{P_{out}}{P_{in}}\right) \qquad (3)$$

Here P_{in} denotes the optical signal power measured at the output of the input fiber before the interconnection, and P_{out} denotes the power at the receiving power after the interconnection is completed. Minimizing the insertion loss is always needed as it directly determines the available system power budget, constrains receiver sensitivity requirements, and governs the maximum transmission reach achievable in amplified or unamplified links.

In SMF-HCF interconnection the insertion loss is not an independent quantity, it is a composite quantity caused by several physical mechanisms [5].

$$IL= L_{overlap} + L_{misalignment} + L_{process} + L_{Fresnel} \quad (4)$$

Here $L_{overlap}$ is the intrinsic loss due to mode-field diameter (MFD) mismatch between the solid-core SMF and the hollow-core fiber, representing the theoretical minimum loss under perfect alignment and zero reflection.

$L_{misalignment}$ accounts for additional loss arising from lateral offset, angular tilt, and longitudinal separation between the fiber endfaces.

$L_{process}$ includes splice-induced losses including microstructural distortion of the HCF cladding (e.g., capillary collapse during fusion splicing) or adhesive inhomogeneity in bonded assemblies.

$L_{Fresnel}$ is the reflection-induced loss at the silica–air interface, contributing approximately 0.16 dB per facet at normal incidence if not mitigated.

It is important to distinguish Insertion Loss from Higher-Order Mode (HOM) excitation. While power coupled to HOMs remains guided within the HCF and does not directly contribute to IL at the junction, it degrades system performance through multipath interference (MPI) and differential mode delay.

Return loss (RL) is the measurement of the portion of optical power reflected back toward the source, and is expressed in decibels. Return loss is vital in laser delivery, coherent communication, quantum systems, and interferometric sensing. In such applications back-reflections can increase noise, destabilize source, or degrade fidelity. In SMF-HCF interconnections, most portion of the back-reflection comes from the silica-air discontinuity at the interface. At normal incidence, the Fresnel reflectance is [15, 16].

$$R = \left(\frac{n_{si} - n_{air}}{n_{si} + n_{air}} \right)^2 \quad (6)$$

Which resembles to a reflection of about 3.5% each facet and is linked with unmanaged parasitic loss.

The return loss mathematically can be given as

$$RL = -10 \log_{10} \left(\frac{P_{refl}}{P_{in}} \right) \quad (7)$$

Here P_{refl} denotes the reflected power, and P_{in} incident power. The research papers reviewed for this review article show that low-reflection interconnections can be produced by employing anti-reflection coatings, angle cleaving, or mode-field adapters that diminish the effective discontinuity at the interconnection. For sensitive applications, return loss more than 40 dB is always preferred.

2.1.3 Misalignment sensitivity and tolerance

The second significant comparison criterion in the literature is the tolerance of alignment. The performance achieved may deteriorate quickly even when the intrinsic overlap limit is good, and the coupling scheme is very sensitive to lateral offset or angular tilt, or to the lateral separation of the axes. This problem is especially acute with SMF-HCF interfaces since the sizes of modes, symmetries of fields, and effective numerical apertures can vary significantly. This is why most experimental studies do not only describe the minimum insertion loss but also the tolerance window within which acceptable performance is ensured. In the review sense, this is not a peripheral point; it is a proxy of manufacturability and field strength. Methods that provide good minimum loss but only at sub-micron alignment criteria can be desirable in the laboratory but challenging to scale. In contrast, marginally more-lossy methods can be more useful in practice when they have a wider alignment tolerance, and are more repeatable.

2.1.4 Higher-order mode excitation and modal purity

The low insertion loss does not ensure a high quality of the interconnection. In most HCF systems, the imperfect launching conditions may drive up the higher-order modes (HOMs) despite the overall transmitted power being reasonable. The outcome can be modal beating, differential mode delay, excessive dispersion, and temporal or spectral variations. Such effects are detrimental especially in coherent connections, long haul transmission, high precision sensing, and interferometric technology. In this vein, modal purity or HOM suppression is becoming an evaluation metric considered in the literature. This is particularly applicable to HCFs, due to their larger cores and structurally complex claddings, they are able to support unwanted mode content much easier than traditional SMFs. Comparatively, a coupling method should then be evaluated on the basis of the amount of power it can transmit, but also on the selectivity with which it can excite the fundamental HCF mode. Sample HOM suppression values below approximately -20 dB are typically desirable, in demanding applications, but acceptable values can vary depending on fiber design and system response.

2.1.5 Effects that are polarization-dependent and prevention of polarization

Polarization behaviour is an additional comparison parameter for SMF-to-HCF interface, specially in coherent transmission, interferometric sensing, gyroscopes, ultrafast laser delivery, and quantum communication systems. Even when insertion loss and back-reflection are low, the interconnection may still degrade performance through polarization-dependent loss (PDL), polarization crosstalk, phase retardance, or imperfect preservation of the input state of polarization. These effects may arise from: (i) structural asymmetry of the hollow-core fiber itself; (ii) stress induced during splicing, tapering, or adhesive curing; (iii) angular misalignment between polarization-maintaining axes; (iv) connector ferrule eccentricity; or (v) environmentally induced bending and twisting.

Zhang et al. demonstrated that polarization preservation can be a decisive metric in PM-HCF/solid-core fiber interconnections, reporting a hybrid two-step splice with approximately 0.7 dB insertion loss, back-reflection below −35 dB, and a polarization extinction ratio (PER) of about 27dB. In practice, PER is measured by launching a linearly polarized source and rotating a polarizer at the output, while PDL is obtained from the maximum and minimum insertion loss across all input polarization states. For polarization-sensitive systems, the polarization extinction ratio (PER, a measure of how well a single linear polarization is maintained) and polarization-dependent loss (PDL, the peak-to-peak variation in insertion loss with input polarization) should therefore be reported alongside insertion loss, return loss, and HOM suppression. At the same time, polarization performance is fiber-dependent: while some modern NANFs exhibit very high intrinsic polarization purity and minimal birefringence, the overall system remains limited by the weakest interconnection or packaging element.

2.2 Thermomechanical and Environmental Stability

Preliminary optical performance is not all that in the assessment. A coupling method that works well in the short-term following the fabrication can be drifting during thermal cycling, vibration, bending, exposure to humidity, or aging. This is of great concern in SMF-HCF interfaces since the joint frequently contains a combination of dissimilar geometries and in certain approaches, other materials such as adhesives, coating, ferrules or micro-optics. Thermomechanical stability is thus assessed in the literature based on insertion-loss drift with temperature, return-loss drift, axial tension resistance, bend tolerance and vibration or hand-to-hand survivability. Local stress or micro bending or partial delamination can be caused by the thermal differential expansion between solid silica regions and micro structured HCF sections. Mechanically speaking, the question at issue is not merely whether the joint is still intact, but whether it still maintains its optical. after environmental loading performance. In the case of a review article, such metrics of stability are necessary since they distinguish those techniques that are optimized to achieve record low loss under controlled conditions compared to those which can be used in real deployment, **where** environmental reliability frequently is as significant as absolute optical efficiency.

2.3 System-level relevance of the reported metrics

Each metric is important depending on the target application. Coherent communication and quantum links, as examples, are very demanding not only in terms of insertion loss or return loss but also in terms of high suppression of HOM excitation.

The high-power delivery is focused on low reflection and good thermal capability, as back-reflection and local heating can cause instability or destruction to the source. Sensing and interferometric detection are especially susceptible to environmental drift and modal interference. In the meantime, field-deployable telecom interconnects must be not only acceptable optical performance, but also process repeatability, packaging compatibility, and repairability. This dependency of applications is the reason why no convergence of literature on one best coupling strategy is realized. Rather, the corresponding comparison is multidimensional: low loss, low reflection, high modal purity, environmental stability, fabrication tolerance, and compatibility with packaging or connectorization have to be weighed against each other.

2.4 Practical metrics for deployment and scale-up

In addition to optical and mechanical performance, yield, reproducibility, cost, and scalability are also highlighted in a number of studies. These are critical in commercializing a laboratory demonstration into a practical interconnection technology. Those methods that rely on the active alignment of the highly optimized or case-specific microstructuring can provide excellent headline performance, but they are not easy to automate. Conversely, techniques that have marginally worse optical characteristics can be more appealing in case they offer greater assembly yield, easier packaging, or easier field replacement. This is why this review considers deployment viability as a valid axis of comparison with optical performance. The most applicable practical indicators are repeatability of the insertion loss and return loss, between samples, standard packaging compatibility, complexity of alignment, repairability, and non-laboratory stability. Section 3 and Section 4 utilises these factors to differentiate between methods that are only high-performing and those that are truly promising to be incorporated into traditional fiber networks.

3. Techniques for Solid-to-Hollow-Core Fiber Coupling

A number of SMF-HCF interconnection techniques have been developed. The most prominent and popular techniques are presented in the following subsections by the couple technique. The reader must, however, understand that the applicability and performance of each of the techniques is highly dependent on the type of hollow-core fiber. As a general roadmap: fusion splicing (including angle-cleaved and offset-spliced variants) works best for photonic bandgap fibers (PBGFs) and some anti-resonant designs but is incompatible with thin-strut nested fibers (NANFs, DNANFs) and Kagome-type fibers unless specialized tapering or GRIN adaptation is employed; tapering (whether of the HCF or SMF) is effective for Kagome and negative-curvature HCFs but challenging for PBGFs; lens-based coupling is universally applicable across all HCF classes (though bulkier); adhesive bonding currently achieves record-low loss only for NANF/DNANF platforms and remains unverified for other classes; and connectorized solutions have been demonstrated primarily for conjoined-tube fibers (CTFs).

3.1 Fusion Splicing to connect SMF to HCF

Fusion splicing is one of the most widely employed technique to permanently join similar to dissimilar fibers . This is achieved by typically melting and fusing the ends of the aligned fibres with an electric arc to create a continuous, lossless path of light as illustrated in Fig. 2. Although, splicing of the same type of fibers is an easy task, the process of interconnecting between the different ones, like, SMFs and the HCFs, creates a great difficulty. Mismatches in structures and modes need to be optimized in parameters and alignment methods that are specific. The main challenge is the basic distinctions between solid- and hollow-core waveguides. Air-filled cores and microstructured cladding used in HCFs make them prone to collapse or deformation due to the heat intensity of a conventional fusion arc. This may lead to higher loss of insertion, back reflection, and higher order mode excitation. Other losses are due to mode-field diameter misalignment and Fresnel reflections in silica-air interface.In order to eliminate these problems, specific approaches are needed. These may involve maximizing arc power and arc duration, specialized splice software and careful core alignment to reduce losses and maintain the hollow-core structure.Even with these difficulties, fusion splicing is a very dependable and lasting interconnection technique. It is widely used in telecommunications networks, high-speed optical communications, fiber-optic sensors and quantum communication systems, where strong and low-loss joint is essential [17, 18]. Standard fusion splicing of SMF to HCF is challenging due to micro-structural collapse; therefore, advanced variants such as angle-cleaved splicing, offset splicing, and the use of intermediate fibers have been developed to mitigate reflections and mode-mismatch, as detailed in this section.

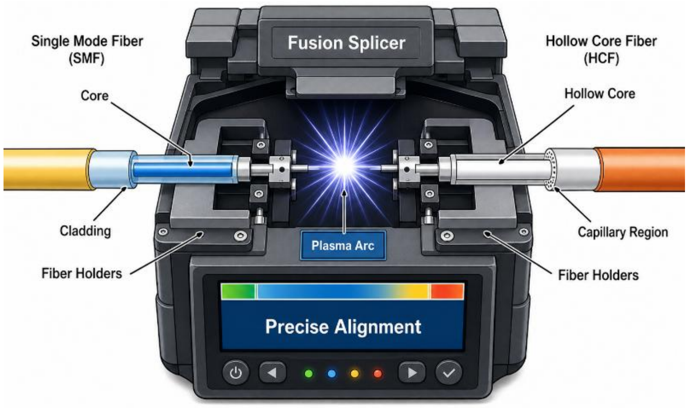

Fig. 2. Fusion splicing of SMF and HCF, showing the plasma arc used for melting and fusing the fiber ends. The alignment process is key to minimizing insertion loss and ensuring a low-loss optical path, with the core, cladding, and capillary region labeled.

Initial attempts by Xiao et al. [19]demonstrated fusion splicing of SMFs into photonic crystal fibers (PCFs) [19]. Nevertheless, a low-loss interconnection was made with back reflection that was very high as a result of the difference in the refractive index. This study highlights the microhole collapse phenomenon when the splicing process is in progress and its effects on splice loss, and provides guidelines on how the fusion parameters can be optimized. The authors studied five types of PCFs with varying core structures and established that the reduction in air hole collapse is significant in minimizing splice loss. In the case of hollow-core photonic crystal fibers (HC-PCFs), careful control of the arc discharge conditions such as current, length, and axial offset is essential to prevent over-collapse of the air holes, which would otherwise lead to high insertion losses (e.g. 1.45 dB, as reported in their experiments). Other techniques that have also been studied include the application of intermediate fibers in PCFs with a large air-filling ratio and repetitive arc discharges in small-core PCFs. The findings offer practical solutions to the integration of PCFs into conventional fiber systems because of the trade-off between mechanical strength and optical characteristics. This experiment contributes to the existing knowledge on PCF-SMF links in general and hollow-core fiber utilization, which requires high-reliability and low-loss splicing methods in specific cases[19].

Angle-cleaved fusion splicing addresses one of the primary limitations of standard fusion techniques: Fresnel back-reflection at the silica-air interface (~3.5% for normal incidence), which generates parasitic Fabry-Pérot resonances that destabilize laser sources and degrade signal integrity in coherent systems. By cleaving the fiber end at an angle of 1°–8° prior to fusion, the reflected light is deflected away from the core, significantly suppressing back-reflection[20]. Zhang et al. [20]developed an optimized angle-cleaved interconnection between a single-mode fiber (SMF) and a nested antiresonant nodeless fiber (NANF, an advanced hollow-core fiber) using a graded-index (GRIN) mode-field adapter (~277 µm optimal length) to compensate for the mode-field diameter mismatch. A rotating CT-105 Fujikura cleaver with a z-adjust stage permitted consistent cleavage angles, with an error of ±0.3°. To prevent microstructure deformation of the NANF during the fusion process, a two-step splicing procedure was adopted: the first step is the weakly bonded arc of high power and short duration, and the second step is the stronger splicing arc of lower power and longer duration, leading to negligible splice loss of less than 0.3dB. The experimental findings showed a loss of connection of approximately 1.25 dB and back-reflection repression of less than -40 dB at a cleave angle of 2.2 °, which is a significant enhancement of the performance of flat-cleaved joints (approximately -15 dB back-reflection). The coupling of the higher-order mode (LP11) was kept below -24 dB, which would guarantee acceptable purity of the mode for most applications (Fig. 3a). The balance between back-reflection suppression (which increases more quickly to an angle of less than 2.5°) and connection loss (which increases almost quadratically with angle) is shown in Fig. 3b with the corresponding quantitative data summarized in Table 1. Back-reflection is minimized at the optimum angle of approximately 2^{o} and connection loss is kept near 1^{o} thus, this regime is very appealing for practical implementation. Although these improvements have been achieved, the method requires specialized cleaving tools and high-precision process control, which means that it is not easily scalable and automated; thus, the method remains an experiment.

The results are also specific to NANF structures operating in the first antiresonant window; extension to other hollow-core fiber designs (e.g., photonic bandgap or different tube geometries) may necessitate further optimization. Overall, angle-cleaved fusion splicing with GRIN adaptation offers a robust, low-cost solution for applications requiring strong back-reflection suppression, such as short-haul high-speed data links and coherent systems; however, continued refinement is needed for broader adoption in long-haul and quantum networks[20].

Table 1. Connection loss and back reflections as a function of GRIN angles [20].

GRIN angle (°)	Calculated connection loss (dB)	Measured Back-reflection (dB)	Back-reflection compared to flat cleaving (dB)
0	0.35	-15	0
1	0.5	-25	10
2	1.0	-41	26
5	4.2	-54	41
8	10.2	-63	48

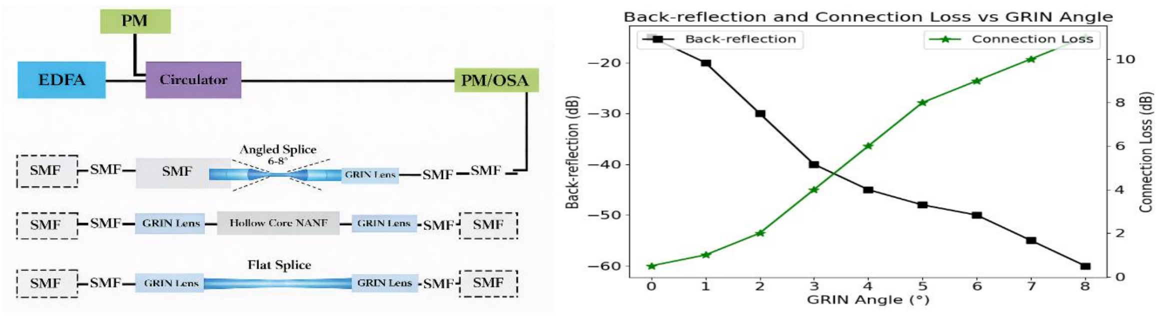

(a) (b)

Fig. 3. Optimized performance and trade-offs in angle-spliced SMF-HCF interconnections using a GRIN mode field adapter. (a) LP11 higher-order mode (HOM) coupling as a function of GRIN cleave angle, demonstrating suppression below -24 dB at ~2.2° (b) Merged plot of back-reflection suppression (decreasing rapidly to below -40 dB at angles near 2.5°) and connection loss (increasing nearly quadratically, maintaining ~1 dB at optimal 2°) vs. GRIN cleave angle, highlighting the balance for low-loss applications[20].

Angle-cleaved fiber splicing is an effective technique for suppressing Fresnel back-reflection, but it introduces beam refraction at the angled glass-air interface. This refraction leads to increased coupling loss and undesirable higher-order mode (HOM) excitation [20]. To overcome this limitation, Shi et al. [21] proposed an offset-splicing method using a gradient-index (GRIN) fiber mode-field adapter. Their approach introduces a deliberate lateral offset between the single-mode fiber (SMF) and the GRIN fiber during fusion splicing.As illustrated in Fig. 4(a), this lateral offset (typically 4–5 µm) pre-shifts the incident beam to compensate for refraction at the angled interface (cleaved at 6–8°). This correction restores on-axis (axial) propagation into the hollow-core fiber (HCF), thereby eliminating the excess loss and HOM excitation associated with angle-cleaving while maintaining high back-reflection suppression (>60 dB reduction)[21].

The performance trade-off of this method is shown in Fig. 4(b). The left y-axis plots coupling loss against the SMF-to-GRIN offset for different cleave angles (0°, 2°, 4°, 6°). For each angle, an optimal offset exists that recovers a low coupling loss of approximately 1–2 dB, matching the performance of a flat cleave. The right y-axis shows the corresponding back-reflection suppression at these optimized offsets, achieving ultralow values below -60 dB (experimentally down to -64 dB) [22]. This demonstrates that offset compensation successfully decouples the traditional trade-off between low back-reflection and low insertion loss [21].

Experimentally, using a 14 m nested antiresonant nodeless fiber (NANF), Shi et al. validated this approach with a 4.5° cleave angle and a 5 µm offset. They reported a pre-arc coupling loss of 0.6 dB, a post-splice loss of 1.2 dB, and a back-reflection of -64 dB [22]. The technique also features low HOM (e.g., LP_{11}) coupling and creates strong, hermetic splices, making it suitable for high-power laser delivery, gas sensing, quantum communication, and temperature-insensitive interferometry.The primary drawbacks are the requirement for sub-micron offset accuracy, specialized alignment equipment, and optimization that is specific to particular HCF types (e.g., NANF in the 1550 nm band). Future work could focus on extending this technique to diverse HCF microstructures and developing automated manufacturing processes to improve scalability [21].

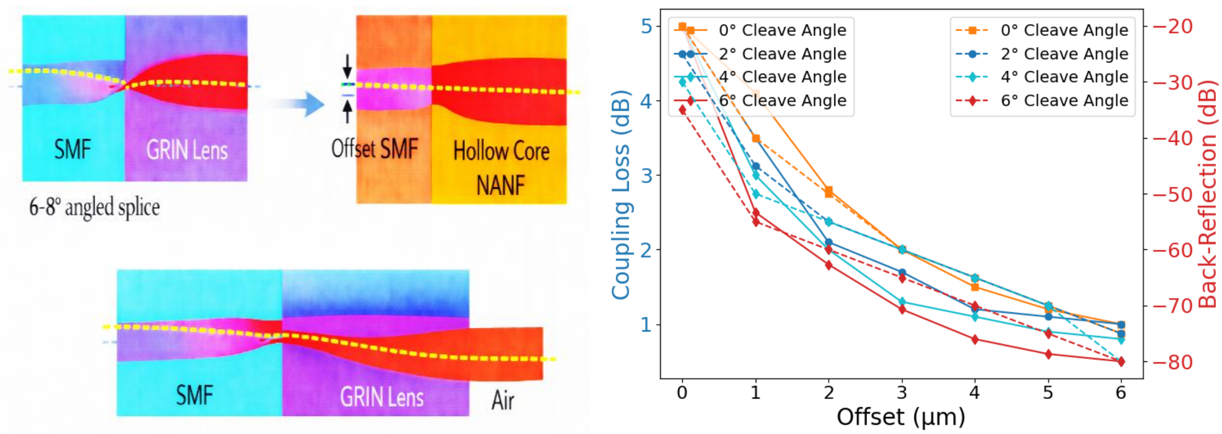

(a) (b)

Fig.4. (a) Operating mechanism of offset-spliced fusion splicing for SMF to hollow-core NANF. The angled cleave (6–8°) suppresses back-reflection, while the intentional lateral offset between SMF and GRIN compensates for refraction at the interface, restoring axial beam propagation and low coupling loss [21]. (b) Performance trade-off in offset-spliced angle-cleaved SMF-HCF interconnections. Left y-axis: Coupling loss (dB) vs. SMF–GRIN offset (µm) for cleave angles 0°–6°, showing optimized offsets restore low loss (~1–2 dB). Right y-axis: Back-reflection suppression (dB) vs. cleave angle at optimized offsets, achieving ultralow values (<-60 dB, down to -64 dB experimentally)[21].

A systematic optimization of the fusion splicing parameters of SMF-to-AR-HCF connections has been performed by Burian et al. [23]using a Fujikura FSM-100P splicer, assessing four different methods: direct fusion with optimized arc parameters, fiber tapering, angle cleaving, and GRIN fiber insertion. In their experiments on direct splicing, a uniform SMF profile gave a total assembly loss of 3.463dB but with systematic optimization of arc power, arc duration and offset on the SMF side the loss could be reduced to about 6 dB per splice. Mode-field matching was made more effective by fiber tapering, decreasing the diameter of the HCF cladding to 35 µm, but increased reproducibility problems and mechanical weakness, with failures always in the tapering section, not at the splice interface itself. Angle cleaving was found to be effective in back-reflection suppression: the largest reported back-reflection of -34.4 dB was at a cleave angle of 10, however at this tradeoff 12.32 dB of insertion loss, so this method may only be applicable to situations where reflection control is more important than loss. The lowest back-reflection was obtained with the insertion of a 1.3 mm GRIN fiber segment (−38.2 dB), but at a high cost of the insertion loss (16.01 dB), indicating that even though GRIN fiber is effective in mode-field adaptation, further optimization is required in order to reduce the loss to realistic levels. In addition to optical performance, Burian et al. determined a number of practical issues in implementation, such as camera misalignment, unstable autofocus at the time of tapering, and the practical constraints of using OTDR measurements in very short fiber lengths. Their contribution highlights the idea that, although consistent SMF-HCF splicing can be achieved through the right optimization strategies, reliability, and mechanical stability are left challenges to industry implementation.

3.2 Tapered fiber coupling for SMF to HCF Interconnection

Tapered fiber coupling mitigates the significant mode-field diameter (MFD) mismatch between SMFs and HCFs by adiabatically transitioning the optical mode [24]. This can be achieved by tapering either the HCF or the SMF.

3.2.1 HCF Tapering

One approach is to taper the HCF end to better match the SMF's mode field. Zheng et al. [25]applied this technique to inhibited-coupling (IC) hypocycloid-core Kagome hollow-core photonic crystal fibers (HC-PCFs). Using vacuum-assisted tapering, they reduced the fiber's outer diameter from 300 µm to 125 µm (a down-taper ratio of 2.4) while preserving the negative-curvature core contour. The strut thickness was reduced from 550 nm to 220 nm over an adiabatic transition length of 5–20 mm. Subsequent collapse of the tapered cladding end via a filament splicer enabled mode-field adaptation. This process achieved a record-low down-taper loss of 0.07 dB at 1550 nm (for a 20 mm transition). The forward-direction (SMF-to-Kagome) insertion loss (IL) was 0.48 dB, with 76.3% of power in the fundamental mode. In contrast, the reverse direction (Kagome-to-SMF) exhibited a higher IL of 3.5 dB due to residual MFD mismatch and significant higher-order mode (HOM) excitation, with 51.1% of power in HOMs (primarily HE_{12}) as confirmed by numerical overlap integrals[25].

This method is particularly effective for unidirectional, high-power laser delivery and nonlinearity-sensitive applications. Its limitations include the need for precise vacuum control to prevent strut buckling, applicability primarily to specific hypocycloid-core designs, and reduced efficiency in bidirectional systems due to HOM generation during the up-taper process. Future studies could explore symmetric tapering profiles or advanced HOM suppression techniques to enhance scalability across a broader range of HCF types[25].

3.2.2 SMF Tapering

Another, complementary method is to taper the end of the SMF itself, adiabatically expanding its mode field to the larger MFD of the HCF without altering the fine delicate microstructure of HCF. This method was first developed by Huang et al. [26]who showed that a low-loss coupling scheme could be achieved between a solid-core SMF and anti-resonant HCFs (AR-HCFs) via a conical fiber taper on the SMF side. As illustrated in Fig. 5, this method is based on the development of a controlled conical taper on the SMF, and scaling the core/cladding diameter down to a tightly optimized waist diameter (usually 6-10 µm). This enables the guided fundamental mode to grow adiabatically, and acquire efficient mode matching with the large core of the AR-HCF with minimal diffraction and reflection losses [26]. Simulations of beam propagation method (BPM) found a trade-off that was optimal, with a coupling loss of about 0.4 dB in an ice-cream-shaped AR-HCF (optimal waist about 8 µm) and 0.8 dB in a node-less AR-HCF (optimal waist about 9 µm). Coupling efficiencies of the ice-cream design were 91.4% at 1.06 µm and 90.2% at 1.57 µm, and the node-less design was 83.7% in anti-resonant transmission windows, which is impressive performance. The SMF-tapering technique is particularly useful in the fabrication of miniature, stable all-fiber systems e.g. mid-infrared fiber gas lasers since the technique avoids the possibility of deforming the microstructure of HCF tapering. Nevertheless, it requires the fine adjustment of the taper profile and the width of the waist because any slight deviation may lead to high loss increments. Moreover, its high performance is design and wavelength dependent and cannot be immediately extrapolated to other types of HCFs, or other spectral ranges. The HCF tapering or advanced taper shaping could be explored in combination with hybrid combinations in the future to enhance efficiency and bandwidth.

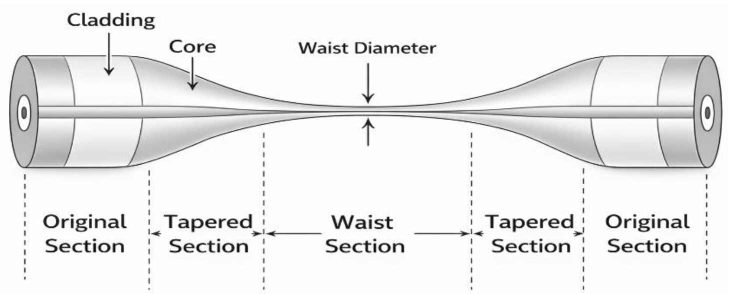

Fig.5. Schematic of the tapered SMF coupling approach to an anti-resonant hollow-core fiber (AR-HCF). The figure illustrates a bi-tapered SMF with a conical waist region that enables adiabatic expansion of the mode field to better match the larger mode-field diameter of the AR-HCF core [26].

3.2.3 SMF Reverse-Tapering for NC-HCFs

A similar method of negative-curvature HCFs (NC-HCFs) was invented by Wang et al.[27]. They used a two-step reverse-tapering procedure of the SMF end to pre-expand and then optimally match the mode profile to the overlap with the NC-HCF core to allow robust direct fusion splicing without intermediate fibres such as graded-index lenses. This simple method had an insertion loss of 0.88 dB at 1310 nm in a complete SMF/NC-HCF/SMF chain[27]. It can be very useful in telecommunications of high capacity, delivery of high power lasers, and sensors with low latency. The first constraints are that the taper parameters (waist diameter and transition length) must be controlled in a specific way, and optimization must be done at a wavelength that can be wavelength-dependent and may require re-engineering to optimize to other operating bands or NC-HCF designs[27].

3.2.4 Tapered No-Core Fiber (TNCF) as a Mode-Field Adapter

Recently, Zhu et al. (2026) reported a combination of tapered single-mode fiber (TSMF) and tapered no-core fiber (TNCF) to enable effective coupling among typical SMF and huge-core anti-resonant hollow-core fibers (ARHCFs) [28]. No-core fiber (NCF) is made of straight silica, lacking a gradient in refractive index, and so light is able to expand or focus, depending on the tapering geometry. In the design, the TNCF is spliced between the ARHCF and a TSMF. The TNCF directs the increased output beam of the large-core ARHCF (core diameter 46.7 μm) to the smaller mode-field diameter of the TSMF (waist diameter of the order of 25 μm). It is a two-step taper design that surpasses the drawback of the traditional SMF tapering, which can rarely open the mode field to more than approximately 25 μm without serious loss. The major benefit of this scheme is that the TNCF is a pure passive mode-field transformer and does not touch the delicate ARHCF microstructure at all--no heat of fusion splicing is put directly on the ARHCF. Using beam propagation method (BPM) simulations, Zhu et al. quantified the performance improvement. With TSMF alone (waist diameter 45 μm), the coupling efficiency reached 84.5% at 1550 nm, compared to only 34.7% for direct SMF-ARHCF coupling without any tapering. However, the TSMF alone cannot further increase efficiency because its maximum achievable mode-field diameter is limited to approximately 25 μm. To overcome this limitation, a TNCF is introduced before the TSMF. With the TSMF fixed at its optimal 45 μm waist diameter, optimizing the TNCF waist diameter to 43 μm improved the coupling efficiency to a peak of 93.5%, corresponding to a total loss reduction of 4.28 dB from the baseline direct coupling. Experimental measurements confirmed a 4.13 dB loss reduction, in excellent agreement with simulations. The residual Fresnel reflection at the ARHCF–TNCF interface contributed approximately 0.3 dB to the total loss, which could be further suppressed by applying anti-reflection coatings.

Beyond its optical performance, this technique offers several practical advantages: (i) the insert coupling approach preserves the HCF microstructure, avoiding heat-induced collapse; (ii) the fabrication process uses standard commercial equipment (hydrogen–oxygen flame tapering machine with flow rates of 8.0 SCCM for oxygen and 110.0 SCCM for hydrogen), enabling reproducibility across laboratories; (iii) the design is compact and robust against cutting errors; and (iv) it is scalable for mass production. These characteristics make the TSMF–TNCF structure particularly promising for high-power laser delivery and low-loss optical coupling in large-core ARHCF systems, where conventional fusion splicing or simple tapering falls short.

3.3 Interconnecting SMF to HCF through connectors

Connector-based coupling methods have important merits, including plug-and-play ability, user-friendliness, scalability, and compatibility with the already available fiber-optic infrastructure, as illustrated in Fig. 6. Connectors can be connected and disconnected many times, unlike more permanent techniques such as fusion splicing or gluing, without damaging the integrity of the fiber; therefore, connectors are useful in field-deployable systems, modular networks, and systems that must often be reconfigured. Conventional connector designs have, however, been challenged by hollow core fibers (HCFs) because of issues such as mismatch of mode-field diameter (MFD) and core non-concentricity, random offsets in ferrules, and Fresnel reflection, which in most cases lead to insertion losses (ILs) in excess of 0.3 dB.

Fig.6. The connection between Standard Single-Mode Fiber (SMF) and Photonic Bandgap Hollow-Core Fiber (HCF) is depicted by this diagram with a commercial SC connector located between the two fibres. The figure shows a high degree of alignment of the fibers by the connector that maintains optimum performance of a low loss transmission.

One innovation step in this direction was made by Zhang et al.[29], who created a more complex connector-like interconnection of HCFs, with a record-low IL and at the same time offering pluggability and robustness. The method employed ceramic ferrules (10.5 mm long) that had a funnel shape to ensure that the glue was applied in the area of the end-face and there was no adhesive entering into the HCF core and to give it a greater mechanical stability. To resolve angular misalignment, which is a critical issue of large-MFD HCFs, they utilized connectors that offer auto-collimation to minimize tilt to less than 0.002 rad, which causes minimal loss (<0.07 dB) based on Gaussian mode analysis. The HCF-to-HCF Conjoined-Tube Fibers (CTF) interconnection experimental setup is shown in Fig. 7. The figure depicts the application of a specially designed metallic mating sleeve with a 3X4 slot layout, which allows it to be rotated by 30 °. This modification makes it possible to reduce transverse offsets, which are due to the non-concentricity of the cores and offsets at the ferrelle. The outcome indicates that there is an IL of minimum 0.13 dB at 1550 nm and the standard deviation of 0.03 dB, over 10 plug-unplug trials. This is the highest record ever made for fusion splicing (0.16 dB) and is close to the theoretical mismatch limit (0.074 dB). Moreover, mode-field adaptation is necessary to overcome the MFD difference (10.4 µm in the case of SMF and 27.9 µm in case of CTF) in the case of HCF-to-SMF (SMF-28) interconnections. Two of the adapters tested by Zhang et al. were the Graded-Index Multimode Fiber (GIF) and Thermally Expanded Core (TEC) SMF. The TEC-based adapter was also superior, with better mode-field matching (its circular mode profile) and with an IL of 0.10 dB at 1489 nm (0.135 dB at 1550 nm), the lowest recorded of any HCF-SMF joint, only 0.03 dB above the theoretical limit based on MFD mismatch. It is an innovative connector-based system that provides a strong connection between HCFs and SMFs at low loss and high efficiency, and is optimally applicable to high-rate communication systems, quantum networks, and other photonic systems [29].

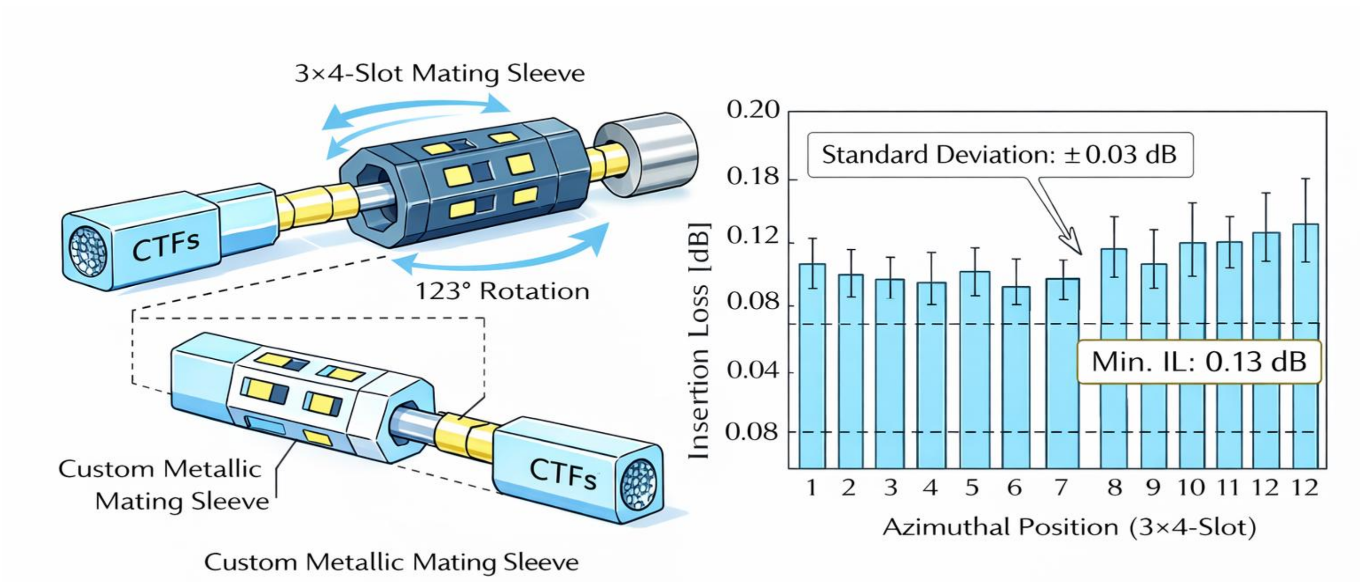

(a) (b)

Fig.7. Connector-based interconnection for Conjoined-Tube Fibers CTFs with custom metallic mating sleeves, illustrating the 12° rotational adjustment for optimal alignment. The bar graph (b) shows the measured insertion loss (IL) across azimuthal positions, with a minimum IL of 0.13 dB and a standard deviation of ±0.03 dB [29].

3.4 Lens-based coupling to couple SMF to HCF

Lens-based coupling is a versatile and flexible method of interconnecting standard SMFs and HCFs. This method solves the inherent problem of MFD differences, in which free-space optics, such as microlenses or graded-index (GRIN) lenses, are used to actively correct and re-direct the optical beam between dissimilar fiber ends, as shown in Fig. 8. Lens-based systems form a collimated or focused beam in an intermediate air gap rather than in direct physical contact or tapering of the fibers themselves. This intermediate beam can be manipulated accurately to maximize mode field matching, alignment tolerance, and optical performance. Its principle is to send the SMF through a lens to expand and focus its tightly focused Gaussian beam and a second lens (or the same lens in an inverted design) to concentrate the beam in the wider fundamental mode of the HCF. The result is a method in which the alignment of the physical fiber is independent of the matching of the optical mode, providing the advantages of reconfigurability, allowing the addition of other optical devices (e.g., filters, isolators), and near-theoretical limits of coupling with little back-reflection. Several implementation strategies have been created based on their unique features. Paired aspheric-based systems are available, such as dual-lenses, which can provide excellent control of beam waist location and diameter, and hence can be optimized specifically for particular modes of HCF. GRIN lens-based coupling with short segments of quarter-pitch GRIN fiber as compact and integrated lens elements was used to efficiently convert the SMF output to the HCF input. Recently, micro-optic systems have been developed as integrated systems that incorporate lenses with alignment ferrules in small hermetic housings that can be deployed in the field. One especially novel type is the direct integration of a silica microball lens into the SMF tip to produce a simple but efficient collimator to couple into a large-core HCF [30]. Such variations have general performance advantages, such as low loss of insertion (usually 0.1–0.5 dB), excellent back-reflection suppression (typically below -60 dB with angled surfaces or anti-reflection coating), broadband operation, and high higher-order mode excitation suppression. Lens-sensed coupling is typically more complicated and heavier than direct fusion splicing but is an essential tool in laboratory prototyping, systems that need to be reconfigured dynamically, as well as in integrating HCFs into complex, extensive optical systems, such as isolators, wavelength-division multiplexers, and quantum communication modules [30].

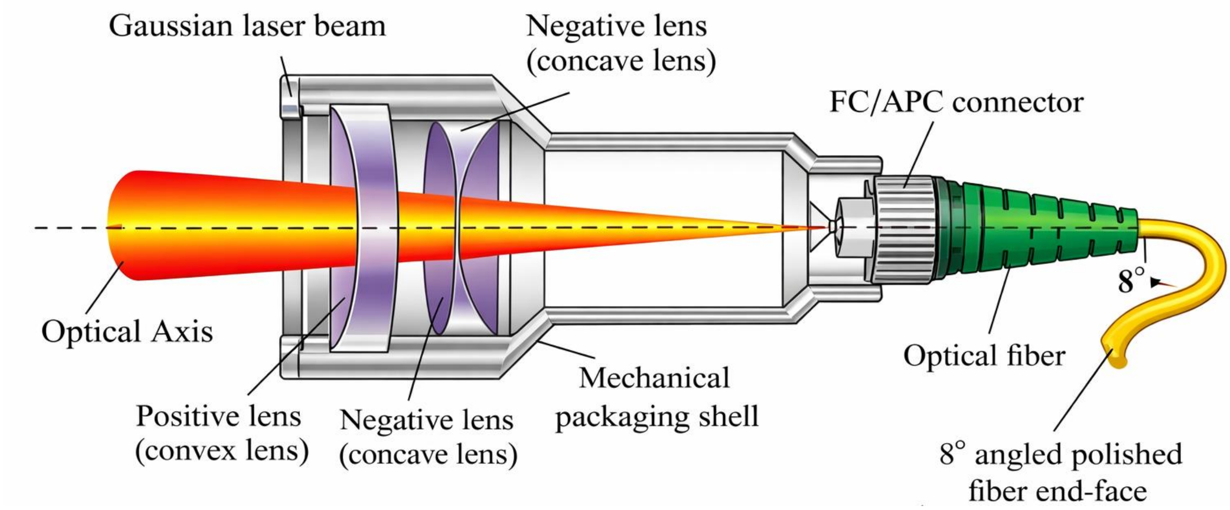

Fig. 8. Lens-Based Coupling in SMF-HCF Interconnections. This diagram illustrates a large-beam fiber coupler featuring double-combined collimating lenses (DCL) and thermally expanded core fibers (TECF), designed to improve optical coupling efficiency between Single-Mode Fiber (SMF) and Hollow-Core Fiber (HCF). The figure highlights the optical path for beam collimation, expansion, and the coupling process, addressing mode field mismatch and alignment challenges commonly encountered in SMF-HCF interconnections[30].

Jung et al. [31]presented a microoptic collimator platform for low-loss interconnections between SMFs) and hollow core fibers (HCFs). This platform enables effective mode-field adaptation between SMF and HCF by adapting the mode-field in GRIN lenses, overcoming the problem associated with mode-field diameter (MFD) mismatch and minimizing back-reflection. Experimental evidence showed that both the LP11 and LP02 modes had low insertion attenuation (0.53-0.58 dB) and low back-reflection (-49.8 dB), with good modal purity and lower higher-order modes (HOMs) (below -20 dB). In Fig. 9(a), a schematic of the experiment is presented, including the collimation of the light coming out of the SMF with the help of a GRIN lens, and the effective coupling of this light into the HCF with the help of a micro-optic collimator. The PBGF presented in Fig. 9(b) is a hollow core with a structure consisting of 19 cells, and the performance of the interconnection, in terms of insertion loss and suppression of back-reflection, was measured at various wavelengths (1510-1680 nm). Fig. 9 (c) shows a summary graph of the main findings as wavelength dependence and azimuthal dependence of insertion loss with the minimum IL of 0.13 dB and standard deviation of 0.03 dB between azimuthal positions[31]. The results indicate the strength of the micro-optic collimator platform, which is a good solution for implementation in high-speed optical communications, quantum networks, and high-power laser delivery, where low loss and low back reflection are essential. In addition, the platform offers trustworthy interconnections in field-deployable systems and demonstrates its potential for use in a broad spectrum of photonic applications. The work of Jung et al. (2019) was further extended to multi-port HCF components, in which they were able to add isolators, band-pass filters, and other useful functional units to the SMF-HCF coupling system with low insertion loss and high stability, even in the long-term[31].

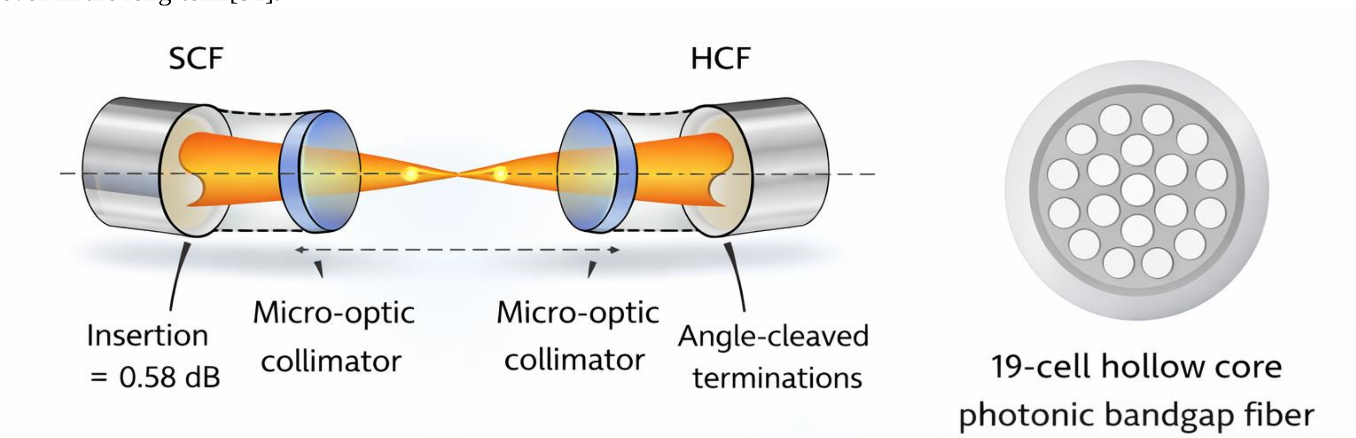

(a) (b)

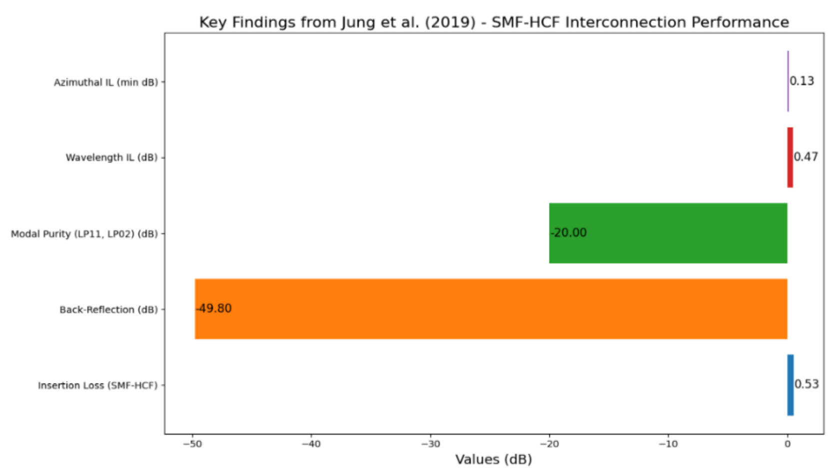

(c)

Fig. 9. An example of the SMF-HCF connection scheme and the essential experiment outcomes of Jung et al. (2019). (a) Diagram of the lens-based coupling system with micro-optic collimators and GRIN lenses to couple light effectively between Single-Mode Fiber (SMF) and Hollow-Core Fiber (HCF). (b) Cross-section of a 19-cell Hollow-Core Photonic Bandgap Fiber (PBGF) used in the interconnection. (c) Major research results: Insertion loss (0.53-0.58 dB), back-reflection suppression (-49.8 dB), and modal purity with little higher-order modes (HOMs) at all wavelengths and azimuthal angles[31].

Addressing the issues of a large core diameter mismatch, Chen et al.[27] suggested a new coupling approach that can increase the coupling efficiency of a large-core hollow-core fiber (LC-HCF) with an SMF. The suggested coupling system consists of a pure silica ball lens attached at the front of the SMF, which focuses the light of the LC-HCF and couples it effectively into the SMF. This is a novel method that is not based on core diameter matching, and it provides a solution to fiber-to-fiber coupling in a situation where there is a large difference in the core diameter, as shown in Fig. 10 (a). The experimental findings showed that 50% efficiency of the coupling was realized with a numerical aperture (NA) of the SMF of 0.22, which is a huge upgrade of the 3.2% level of the coupling efficiency realized when using direct coupling techniques. The study also placed special emphasis on the fact that the NA of the SMF has a direct positive effect on the coupling efficiency, and the maximum efficiency of the coupling is attained at NA = 0.22, as shown in Fig. 10 (b). This increased the insertion loss to approximately 3 dB, which is a significant decrease compared with the insertion loss of 15 dB, which is normally experienced with a direct coupling technique. Optical feedback was also minimized by suppressing back reflection. This scheme is an efficient and flexible coupling scheme that is useful in a variety of applications, such as optical communications, high-power laser delivery, and nonlinear optics, where a high coupling efficiency is required[27].

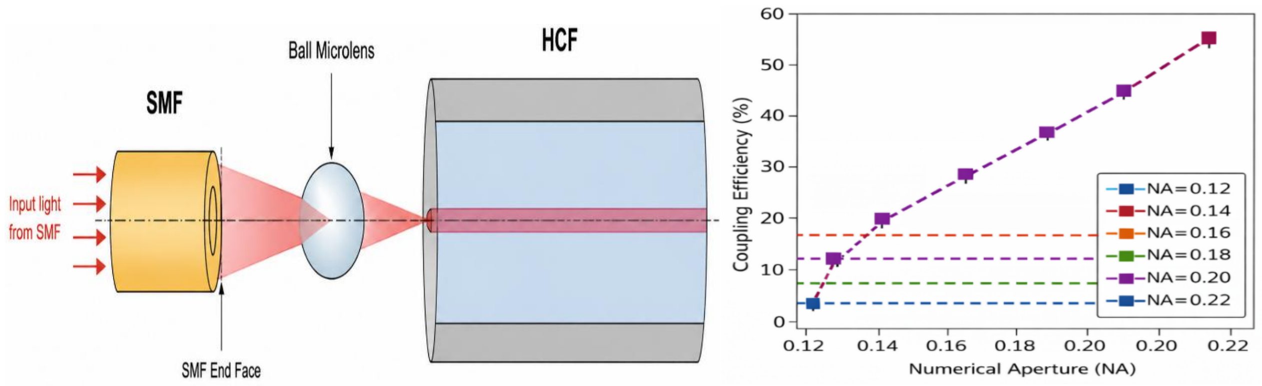

(a) (b)

Fig. 10. Performance of the coupling between LC-HCF and SMF on a new coupling structure. (a) Diagram of the connection arrangement, with the pure silica ball lens at the front-end of the SMF, which will be designed to focus the light that is produced by the LC-HCF to the SMF core. (b) Numerical Aperture (NA) vs. Coupling efficiency illustrating the rise in the efficiency with higher values of NA, reaching a 50 percent coupling efficiency at NA = 0.22 [27].

3.5 Bridge Splicing Techniques: Photonic Crystal Fiber (PCF) and Gradient-Index Fiber (GIF) Intermediaries

Directly splicing standard single-mode fibers (SMFs) to specialty fibers like Photonic Crystal Fibers (PCFs) or Hollow-Core Fibers (HCFs) is challenging due to significant mode-field diameter (MFD) and structural mismatches, often resulting in splice losses exceeding 3 dB. Bridge splicing techniques address this by using a short, specially designed intermediate fiber to facilitate an adiabatic mode transition, enabling low-loss and robust interconnections.

3.5.1 PCF Bridge Splicing

Photonic Crystal Fibers (PCFs) are characterized by a microstructured cladding of air holes, offering unique properties such as low nonlinearity, high birefringence, and tailorable dispersion. PCF bridge splicing utilizes a short section of a custom-designed PCF as an intermediary. The geometry of this bridge PCF—its air-hole size, pitch, and arrangement—is engineered to provide a gradual transition between the MFD and effective index of the SMF (e.g., ~10 µm at 1550 nm) and that of the target PCF, which can range from ~2-6 µm for solid-core PCFs to much larger values for hollow-core varieties.

The splicing process requires a high-precision fusion splicer to ensure alignment and employs low-power, controlled arc discharges to prevent the collapse of the delicate air-hole structure, which is critical for maintaining guiding properties. Techniques like offset splicing or short-duration arcs are often used to minimize heat exposure. With a typical bridge length of 1–5 mm, this method has reported splice losses of 0.3–0.5 dB at 1550 nm, a significant improvement over direct splicing.

While offering superior mechanical strength (often exceeding 100 kpsi) compared to adhesive-based methods, PCF bridge splicing presents challenges. The required heat control is delicate, as excess heat can collapse the air holes. Furthermore, fabricating the custom bridge PCF with high structural accuracy involves complex and costly fiber-drawing processes. Despite these hurdles, the technique is vital for integrating PCF-based devices—such as high-power fiber laser components or optical sensors—into standard SMF-based systems.

3.5.2 GIF Bridge Splicing for HCF Interconnection

A conceptually similar but distinct approach for connecting SMFs to Hollow-Core Fibers (HCFs) employs a Gradient-Index Fiber (GIF) as the intermediary bridge. Zhang et al. [32]demonstrated this technique to address the MFD mismatch between a standard SMF (SMF-28) and an anti-resonant hollow-core fiber (AR-HCF), achieving notably lower loss than direct splicing methods.

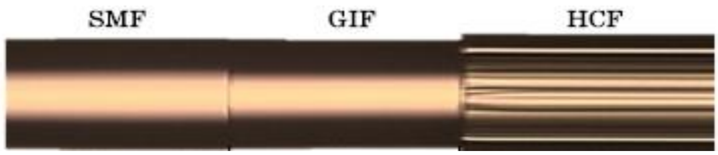

Fig.11. Image of SMF to HCF interconnection, with GIF length 251μm, which has the minimum loss 0.42 dB and least among all [32]

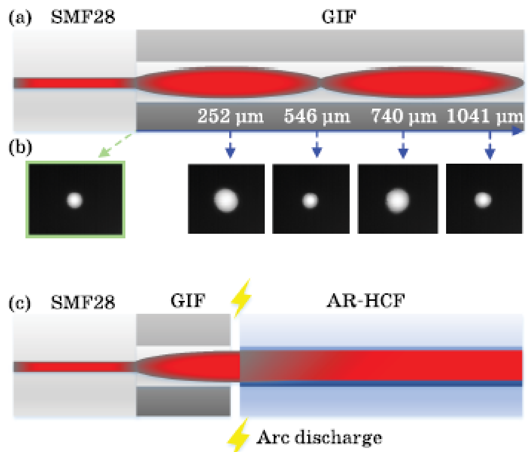

Fig. 12.The diagram illustrates (a) the transmission of light through the used GIF, (b) the mode field images obtained with varying lengths of the GIF, and (c) a schematic representation of the MFD adaption and fusion splicing technique [32].

The core principle, illustrated in Fig. 12, involves using a short segment of GIF to adapt the mode field. Figure 12(a) shows the light transmission path, (b) displays mode field images for different GIF lengths, and (c) schematizes the MFD adaptation and fusion splicing process. The GIF's varying refractive index profile allows the optical mode to expand or contract adiabatically over a precisely controlled length, optimizing overlap with the HCF core.

The performance of this method is highly dependent on the GIF length. Table 2 presents the measured coupling loss at 1550 nm for different GIF pigtail lengths, with an optimal length of 251 µm yielding a coupling efficiency of 90.8% and a minimum loss of 0.42 dB.

Table 2. Measured Coupling Loss (at 1550 nm) from SMFs with Different GIF Pigtail Lengths to the HCF[32].

Length of GIF (um)	**Coupling efficiency (%)**	**Loss in dB**
246	89.9	0.46
251	90.8	0.42
256	87.4	0.58
257	87.1	0.59

Figure 12 provides visual confirmation of the splice quality, showing an optical microscope image of the interconnection with a 251 µm GIF length, which corresponded to the minimum loss. The image reveals a clean, well-aligned joint with minimal deformation of the hollow-core structure, corroborating the low-loss results.

While the GIF bridge method provides a valuable degree of freedom for optimization and significantly reduces loss compared to direct splicing, limitations remain. These include residual mode-field mismatch, the risk of microstructural changes in the HCF from the splicing arc, and the need for precise, case-specific calibration of the GIF length, which may not generalize easily to other HCF types.

3.6 Gluing or Adhesive Bonding

Gluing or adhesive bonding provides a permanent, low-temperature alternative to fusion splicing for interconnecting single-mode fibers (SMFs) and hollow-core fibers (HCFs), preserving the delicate HCF microstructure from heat-induced deformation. This method involves the precise alignment of fiber ends followed by bonding with UV-curable or epoxy adhesives, often incorporating mode-field adapters (MFAs) such as graded-index (GRIN) multimode fibers or thermally expanded core (TEC) fibers to mitigate mode-field diameter (MFD) mismatch.

A benchmark demonstration is provided by Suslov et al. [33], who achieved a record-low insertion loss of 0.15 dB (rising to 0.16 dB post-gluing) between a standard SMF and a nested antiresonant nodeless fiber (NANF), only 0.07 dB above the theoretical minimum due to residual mode shape and symmetry mismatches. Utilizing GRIN-based MFAs to adapt the ~10.4 µm MFD to the >20 µm mode of the NANF, they incorporated an anti-reflection (AR) coating at the interface, suppressing back-reflection below -40 dB over a 60 nm bandwidth while reducing insertion loss by an additional 0.15 dB. The theoretical foundation for this near-optimal performance is shown in Fig. 13, which plots the coupling loss between the GRIN output and the NANF fundamental mode (accounting for its non-Gaussian profile and six-fold symmetry) as a function of GRIN length, revealing a minimum of 0.08 dB with excellent tolerance to length variations (~50 µm). Higher-order mode (HOM) excitation was minimized to <-35 dB for the LP_{11} mode (limited by NANF asymmetry) and <-22 dB for the LP_{02} mode, as confirmed through simulations and spectral analysis. An alternative TEC-based MFA yielded a 0.21 dB insertion loss with comparable HOM suppression. The gluing process, employing a viscous UV-curable adhesive in fiber-array holders, ensured mechanical stability and hermetic sealing without performance degradation, rendering it suitable for high-power lasers, interferometry, and telecommunications [33].

Specificity of adhesive bonding performance in terms of fiber-class. It should be mentioned that the record low insertion losses obtained by Suslov et al. [33] and Zhong et al. [34] were obtained with nested antiresonant nodeless fiber (NANFs) and double-nested antiresonant nodeless fiber (DNANFs) in particular. These fiber designs have fairly strong anti-resonant cladding geometries and mode-field profiles that are resonant to GRIN-based mode-field adapters. It is still unclear whether similar sub-0.1 dB losses are possible with other families of HCFs (including photonic bandgap fibers (PBGFs) with their periodic cladding structures, Kagome-type fibers (with their thin, easily-deformed struts), negative-curvature HCFs (NC-HCFs), or conjoined-tube fibers (CTFs)). The geometry of the cladding, the strut thickness, mode field symmetry, and thermal sensitivity are structural differences that can have various constraints on adhesive bonding. As an example, PBGFs can be more sensitive to adhesive wicking into their periodic air-hole patterns whereas Kagome fibers can be cured at reduced temperatures to prevent strut deformation. Thus, although gluing can be a very promising method in NANF/DNANF interconnections, the efficacy of gluing with other types of HCF needs to be experimentally verified. Those who use adhesive bonding to non-NANF HCFs are also urged to document their findings in a descriptive manner, such as fiber geometry, adhesive type, curing conditions, and degradation mechanisms.

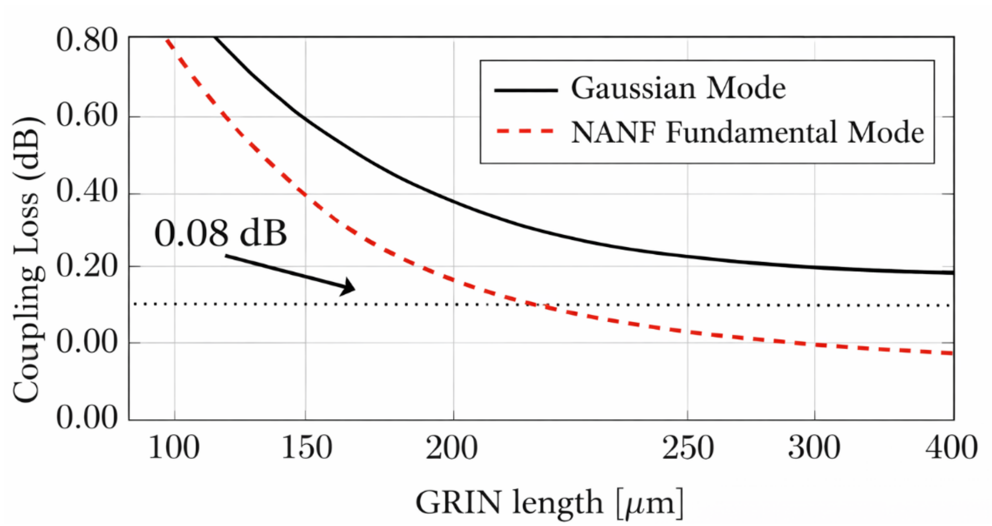

Fig. 13. Theoretical coupling loss (dB) versus GRIN length (µm) between the GRIN MFA output and (solid line) a Gaussian mode approximation, and (dashed line) the actual NANF fundamental mode. The minimum loss is 0.08 dB, with the arrow indicating robust tolerance to GRIN length variations [33].

Subsequent advancements by Zhong et al. [34]refined this gluing strategy to achieve perfect mode-field size adaptation, with experimental insertion losses matching theoretical predictions for the first time. Using tailored GRIN MFAs, they realized a minimum permanent insertion loss of 0.079 dB, stable over 4 weeks of continuous monitoring, across three low-loss HCF variants: first-window NANF, second-window NANF, and state-of-the-art double NANF (DNANF). This breakthrough validated the accuracy of finite-element simulations for arbitrary HCF core sizes, enabling future design optimization without extensive trial-and-error fabrication. The connections also exhibit excellent HOM suppression, mitigating multipath interference in sensitive applications[34].

Although gluing offers superior loss performance, modal purity, and compatibility with AR coatings compared to thermal methods, potential challenges include preventing adhesive wicking into the hollow core and managing thermal expansion mismatches during environmental cycling. Nonetheless, its proven scalability and low-temperature nature make it a leading candidate for integrating HCFs into quantum networks, gas sensors, and high-capacity communication systems.

3.7 Summary of the Reviewed Coupling Techniques

The coupling methods discussed above—ranging from fusion splicing and tapering to lens-based, connectorized, and adhesive-based approaches—each present distinct trade-offs in terms of insertion loss, back-reflection suppression, mechanical robustness, and scalability. To provide a consolidated overview, Table 3 summarizes the key findings from the major studies reviewed in this work, organized by reference number for clarity and ease of reference.

Table 3. Summary of the major papers reviewed in this paper.

Ref. No.	Connection Technique	Types of Fiber	Key Innovation	Remarks
[19]	Fusion Splicing	SMF to HC-PCF	Microhole collapse analysis and parameter optimization	Studied fusion splicing of PCFs to SMFs, highlighting air-hole collapse effects and guidelines for low-loss splicing.
[20]	Angle-Cleaved Fusion Splicing	SMF to nested antiresonant nodeless fiber	GRIN mode-field adapter with angled cleave	Achieved 1.25 dB connection loss and <−40 dB back-reflection at 2.2° cleave angle.
[21]	Offset-Spliced Fusion Splicing	SMF to NANF	Lateral offset compensation for angled cleave	Achieved 1.2 dB splice loss and −64 dB back-reflection with 4.5° cleave and 5 µm offset.
[25]	Fusion Splicing with HCF Tapering	SMF to hypocycloid-core Kagome HCF	Vacuum-assisted tapering of Kagome HCF	Achieved 0.48 dB forward insertion loss at 1550 nm, with low HOM excitation.
[26]	Tapered Fiber Coupling	SMF to AR-HCF	Conical taper on SMF for mode expansion	Coupling efficiency >90% for ice-cream and nodeless AR-HCFs at 1.06 µm and 1.57 µm.
[35]	Reverse-Tapering Fusion Splicing	SMF to NC-HCF	Two-step reverse tapering on SMF	Achieved 0.88 dB insertion loss in SMF/NC-HCF/SMF chain at 1310 nm.
[29]	Connector-Based Coupling	SMF to CTF (HCF)	Custom metallic mating sleeve for alignment	Achieved minimum insertion loss of 0.13 dB with ±0.03 dB deviation.
[31]	Lens-Based Coupling with GRIN Lenses	SMF to HCF (PBGF)	Micro-optic collimator platform	Achieved insertion loss of 0.53–0.58 dB and back-reflection suppression of −49.8 dB.
[27]	Silica Ball Lens Coupling	SMF to LC-HCF	Pure silica ball lens at SMF tip	Achieved 50% coupling efficiency with NA = 0.22, improving from 3.2% in direct coupling.
[32]	GIF Bridge Splicing	SMF to AR-HCF	Gradient-index fiber as intermediary	Achieved 0.42 dB coupling loss with 251 µm GIF length.
[33]	Gluing with GRIN Mode-Field Adapter	SMF to HCF (PBGF, NANF)	AR coating and GRIN MFA for low loss	Achieved 0.15 dB insertion loss (0.07 dB above theoretical limit) and <−40 dB back-reflection over 60 nm bandwidth.
[34]	Gluing with GRIN Fibers	SMF to DNANF and NANF	Ultra-low loss with stable glued connection	Achieved record-low 0.079 dB insertion loss, stable over four weeks.
[23]	Direct fusion, tapering, angle	SMF to AR-HCF	Systematic parameter optimization of four splicing methods	Achieved −34.4 dB back-reflection at 10° cleave (12.32 dB IL); GRIN gave −38.2

	cleaving, GRIN insertion			dB RL (16.01 dB IL); identified reproducibility challenges
[28]	Tapered SMF + tapered no-core fiber (TNCF)	SMF to large-core ARHCF (46.7 µm core)	TNCF as mode-field adapter focusing ARHCF output to match TSMF	Achieved 93.5% coupling efficiency (4.28 dB loss reduction) at 1550 nm; preserves HCF microstructure; scalable and robust against cutting errors

4. Comparisons of Interconnection Techniques

Table 4 synthesizes the performance and trade-offs of the main SMF-to-HCF coupling techniques.. One of the lessons is that gluing/adhesive bonding is currently the lowest insertion loss (down to 0.079 dB), and connector-based connections are right behind (around 0.10 dB). These methods take advantage of mode-field adapters (MFAs) and the anti-reflection (AR) surfaces, which reduce Fresnel reflections and mode-mismatch losses. Fusion splicing and tapered fiber coupling have strong all-fiber solutions, but are usually more prone to losses (0.31025 dB) and back-reflection unless angle cleaving or sophisticated tapering is used. Lens-based coupling is very flexible and modal pure but less practical in compact and field-deployable systems because of its size and sensitivity to alignment. PCF bridge splicing is a useful bridge solution to connect photonic crystal fibers, but not to the ultralow loss levels of gluing or connectorized solutions. This order of performance of insertion losses is plotted in Fig. 14 directly. The final decision about the interconnection technique is based on the application-specific needs, such as acceptable loss budget, must be reconfigurable, environmental, and scalable. An example is that ultralow-loss quantum links might favor gluing to AR-coated MFAs, but field-deployable telecom modules might prefer connector-based approaches to their plug-and-play nature. The next steps will probably be hybrid solutions, automated alignment solutions, and enhanced thermal stability to close the performance gap between laboratory demonstrations and commercial applications.

Table 4. Comparison of HCF to SMF interconnection techniques: performance characteristics and applications.

Technique	Working Principle	Advantages	Disadvantages	Performance Metrics	Applications
Fusion Splicing	Direct arc fusion of SMF to HCF	Simple, compact, robust	High reflections (~0.16 dB loss), risk of HCF collapse	Loss: 0.3–1 dB Reflection: ~−14 dB	Telecom networks, fiber lasers
Connector Based Coupling	Passive alignment via fiber connectors (e.g., FC/PC)	Reusable, no thermal damage	Unsealed, alignment drift	Loss: ~0.5 dB	Lab environments, test setups
Tapered Fiber Coupling	SMF tapered to match HCF mode-field diameter (MFD)	Low reflections (−27 dB), adaptable MFD	Fragile, complex fabrication	Loss: ~0.2 dB Bandwidth: 390 nm	High-power laser delivery, gas sensing
PCF Bridge Splicing	Intermediate PCF segment between SMF and HCF	MFD adaptation, reduced reflections	Complex splicing	Loss: ~0.15 dB	Specialty fiber systems, sensing
Lens-Based Coupling	Air-gap coupling with GRIN/C-lenses	Low loss (0.5 dB), hermetic, low	Bulkier than splicing	Modal purity: >20 dB	Optical isolators,

		reflection (<−45 dB)			filters, WDM systems
Gluing Technique	Permanent bonding with UV epoxy/adhesives	Hermetic seal, stable (<0.01 dB drift)	Irreversible, glue RI optimization needed	Record-low loss: 0.079 dB	Aerospace, harsh environments, medical fiber systems
Free-Space Coupling with Adaptive Optics	Free-space optics with mirrors/lenses for beam shaping	Flexible MFD tuning, minimal fiber damage	Alignment-sensitive, bulky	Loss: <0.1 dB (with active alignment)	Quantum optics, precision alignment systems

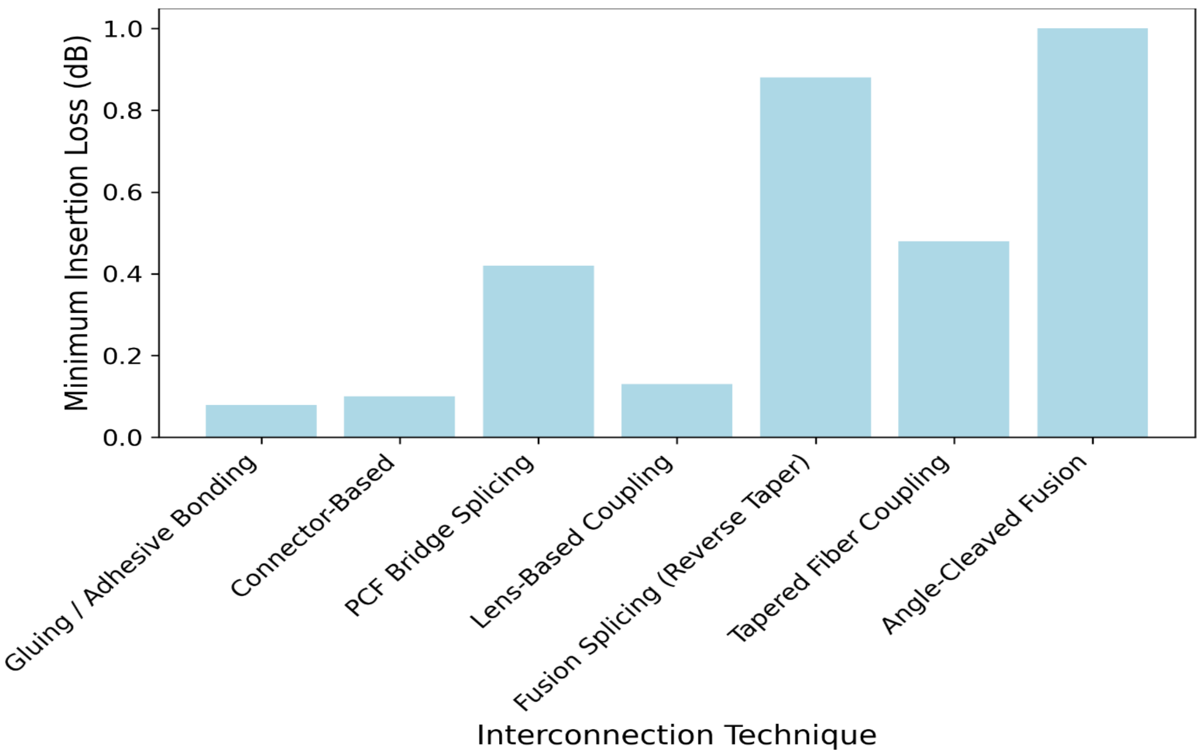

Fig. 14. The insertion loss of interconnection techniques reviewed above.

5. Conclusion

The integration of hollow-core fibers (HCFs) into traditional solid-core fiber networks must be achieved with minimal optical loss. This review systematically compares the leading coupling methodologies, including fusion splicing, fiber tapering (including the novel tapered no-core fiber method), lens systems, connectors, bridge splicing, and adhesive bonding. Each technique presents distinct trade-offs in terms of insertion loss, back-reflection suppression, modal purity, polarization handling, mechanical robustness, and deployability. A key observation is that no single method is universally applicable to all classes of HCFs. The effectiveness of each technique depends significantly on the specific fiber family, such as photonic bandgap (PBGF), Kagome, nested anti-resonant nodeless fibers (NANF), double-nested anti-resonant nodeless fibers (DNANF), negative-curvature HCFs (NC-HCF), or conjoined-tube fibers (CTF). Extrapolating results from one fiber class to another without proper validation should be avoided.

For NANFs and DNANFs, mode-field adapters bonded with adhesives set the standard for ultralow loss (0.079 and 0.15 dB) and excellent back-reflection suppression. However, these results have only been validated for NANF/DNANF platforms; further validation is required for other HCF classes. In polarization-sensitive NANF systems, hybrid splicing achieves an insertion loss of approximately 0.7 dB and a polarization extinction ratio (PER) of 27 dB. More recent designs have reached a PER >21 dB with losses of less than 1 dB per meter. Lens-based coupling (0.53–0.58 dB loss, -49.8 dB return loss) and HCF tapering (0.48 dB forward loss) have been demonstrated to work well with PBGFs and Kagome fibers, while adhesive bonding and direct fusion splicing have not been extensively tested or remain problematic in some contexts.

Tapered fiber coupling, whether via SMF-side tapering (with >90% efficiency), reverse tapering (0.88 dB loss), or the new tapered no-core fiber approach (93.5% efficiency, 4.13 dB loss reduction), is robust. For CTFs, connector-based coupling has 0.10–0.13 dB loss, offering high repeatability and suitability for field-deployable systems. In addition to optical performance, practical considerations such as yield, reproducibility, alignment tolerance, and field repairability are crucial for successful deployment.

Future research directions include: (i) extending adhesive bonding techniques to a broader range of HCF classes, (ii) automating splicing and tapering procedures, (iii) developing temperature-insensitive anti-reflection surfaces, (iv) standardizing polarization and higher-order mode handling, and (v) advancing hybrid methods that combine the advantages of multiple coupling techniques. Overcoming such challenges, especially the necessity of fiber-class-specific validation and scalable production, smooth HCF integration will open the door to high-capacity, low-latency, and nonlinearity-resistant optical networks. These findings lay the groundwork for the next generation of optical fiber networks, with significant applications in 6G and quantum communication systems.

Funding: This research was partially financed by the National Key Research and Development Program of China Project (project ID: 2022YFF0708801) and financed by the Fujian Provincial Natural Science Foundation Project (project ID: 2024J011540,2024CT018).

Conflict of Interest: The authors declare that there is no conflict of interests.

Data Availability Statement: The data that supports the findings of this study are available within the article.

Author Contribution Statement:

Muhammad Hanif Ahmed Khan Khushik: Conceptualization, Project administration, Writing – original draft, Writing – review & editing.

Shahzadi Bano: Data curation, Formal analysis, Writing – original draft, Visualization.

Luo Yinsheng: Investigation, Methodology, Writing – review & editing.

Lu Sun: Resources, Validation, Writing – review & editing.

Guoping Chen: Formal analysis, Investigation, Writing – original draft.

Jamal N.A. Hassan: Writing – review & editing, Visualization, Data curation.

Muhammad Saleem: Methodology, Validation, Writing – review & editing.

Mian Muhammad Kamal: Data curation, Formal analysis, Writing – original draft.

Hamedalneel B A Hamid: Writing – original draft, Investigation, Visualization.

Tianjun Ma: Conceptualization, Funding acquisition, Supervision, Writing – review & editing, Project administration.

References

1. Agrell, E., et al., Roadmap of optical communications, Journal of optics. 18,6 (2016). https://doi.org/10.1088/2040-8978/18/6/063002.
2. Kadhim, A.C., S.H. Al-Ithawi, and A.S. Azzahrani, Orbital angular momentum multiplexing architecture for OAM/SDM passive optical networks, Journal of the European Optical Society-Rapid Publications. 20,2 (2024). https://doi.org/10.1051/jeos/2024027.
3. Macedo, L., et al., Rayleigh scattering-based distributed sensing in multicore optical fibers for shape reconstruction in multiplanar disturbance, Measurement. 256 (2025). https://doi.org/10.1016/j.measurement.2025.118101.
4. Saiyyed, R., et al., Free space optical communication system: A review of practical constraints, applications, and challenges, Journal of Optical Communications. 46,2 (2025). https://doi.org/10.1515/joc-2024-0011.

5. Beatty, R.W., Insertion loss concepts, Proceedings of the IEEE. 52,6 (2005). https://doi.org/10.1109/PROC.1964.3047.
6. Hong, Y., et al., Beyond terabit/s/λ nonlinearity-free transmission over the hollow-core fiber, Journal of Lightwave Technology, (2025). https://doi.org/10.1109/JLT.2025.3533297.
7. Hong, Y., et al., Low-Latency WDM Intensity-Modulation and Direct-Detection Transmission Over> 100 km Distances in a Hollow Core Fiber, Laser & Photonics Reviews. 15,9 (2021). https://doi.org/10.1002/lpor.202100102.
8. Ren, N., et al., Design of subwavelength optical fibre for low-loss Terahertz transmission, Journal of the European Optical Society-Rapid publications. 8 (2013). https://doi.org/10.2971/jeos.2013.13068.
9. Liu, X., et al., Ultra-high capacity transmission in anti-resonant hollow core fiber, Journal of Lightwave Technology, (2025). https://doi.org/10.1109/JLT.2025.3600818.
10. Poletti, F., M.N. Petrovich, and D.J. Richardson, Hollow-core photonic bandgap fibers: technology and applications, Nanophotonics. 2,5-6 (2013). https://doi.org/10.1515/nanoph-2013-0042.
11. Borzycki, K. and T. Osuch, Hollow-core optical fibers for telecommunications and data transmission, Applied Sciences. 13,19 (2023).
12. Ferreira, M.F.S. and M.C. Paul, *Specialty Optical Fibers: Materials, Fabrication Technology, and Applications* (Elsevier,2024).
13. He, L., H.P. Chan, and B. Li, Quantitative study in coupling loss reduction under a large mode-field mismatch using a self-written waveguide, Optics Express. 29,22 (2021). https://doi.org/10.1364/OE.435175.
14. Neumann, E.-G., *Single-mode fibers: fundamentals* (Springer,2013).
15. Shlyagin, M., R.M. Manuel, and Ó. Esteban, Optical-fiber self-referred refractometer based on Fresnel reflection at the fiber tip, Sensors and Actuators B: Chemical. 178 (2013). https://doi.org/10.1016/j.snb.2012.12.092.
16. Xu, W., X.G. Huang, and J.S. Pan, Simple fiber-optic refractive index sensor based on fresnel reflection and optical switch, IEEE Sensors Journal. 13,5 (2012). https://doi.org/10.1109/JSEN.2012.2236751.
17. Wang, C., et al., Ultralow-loss fusion splicing between antiresonant hollow-core fibers and antireflection-coated single-mode fibers with low return loss, Optics Letters. 48,5 (2023). https://doi.org/10.1364/OL.481190.
18. Wei, X., et al., Extraction of Attenuation and Backscattering Coefficient along Hollow-Core Fiber Length Using Two-Way Optical Time Domain Backscattering, ACS Photonics. 11,10 (2024). 10.1021/acsphotonics.4c00859.
19. Xiao, L., et al., Fusion splicing photonic crystal fibers and conventional single-mode fibers: microhole collapse effect, Journal of lightwave technology. 25,11 (2007). https://doi.org/10.1109/JLT.2007.907787.
20. Zhang, C., et al., Angle-spliced SMF to hollow core fiber connection with optimized back-reflection and insertion loss, Journal of Lightwave Technology. 40,19 (2022). https://doi.org/10.1109/JLT.2022.3186721.
21. Shi, B., et al., Splicing hollow-core fiber with standard glass-core fiber with ultralow back-reflection and low coupling loss, ACS photonics. 11,8 (2024). https://doi.org/10.1021/acsphotonics.4c00677.
22. Foroni, M., et al., Guiding properties of silica/air hollow-core Bragg fibers, Journal of lightwave technology. 26,13 (2008). https://doi.org/10.1109/JLT.2007.913692.
23. Burian, R., et al., Fusion Splicing Technique for Minimizing Insertion Loss and Back Reflection Between Single-Mode and Hollow-Core Fibers, Fiber and Integrated Optics. 45,2 (2026). 10.1080/01468030.2026.2629781.
24. Khushik, M.H.A.K., et al., Photonic Nanojet-Enabled Mode Matching for Ultralow-Loss Hybrid Fiber Interconnects, IEEE Photonics Journal, (2026). https://doi.org/10.1109/JPHOT.2026.3658357.
25. Zheng, X., et al., Fusion splice between tapered inhibited coupling hypocycloid-core Kagome fiber and SMF, Optics Express. 24,13 (2016). https://doi.org/10.1364/OE.24.014642.
26. Huang, W., et al., Low-loss coupling from single-mode solid-core fibers to anti-resonant hollow-core fibers by fiber tapering technique, Optics express. 27,26 (2019). https://doi.org/10.1364/OE.27.037111.

27. Chen, X., et al., High coupling efficiency technology of large core hollow-core fiber with single mode fiber, Optics Express. 27,23 (2019). https://doi.org/10.1364/OE.27.033135.
28. Zhu, X., et al., Enhanced coupling efficiency in single-mode to anti-resonant hollow-core fiber systems using tapered no-core fiber, Optical Fiber Technology. 99 (2026). https://doi.org/10.1016/j.yofte.2026.104615.
29. Zhang, Z., et al., Connector-style hollow-core fiber interconnections, Optics Express. 30,9 (2022). https://doi.org/10.1364/OE.456392.
30. He, Q., et al., Optical coupling efficiency of a coupler with double-combined collimating lenses and thermally expanded core fibers, Micromachines. 13,2 (2022). https://doi.org/10.3390/mi13020324.
31. Jung, Y., et al., Compact micro-optic based components for hollow core fibers, Optics express. 28,2 (2020). https://doi.org/10.1364/OE.28.001518.
32. Zhang, Z., et al., Fusion splicing of hollow-core to standard single-mode fibers using a gradient-index bridge fiber, Journal of Optical Technology. 90,1 (2023). https://doi.org/10.1364/JOT.90.000042.
33. Suslov, D., et al., Low loss and high performance interconnection between standard single-mode fiber and antiresonant hollow-core fiber, Scientific Reports. 11,1 (2021). https://doi.org/10.1038/s41598-021-88065-2.
34. Zhong, A., et al., Connecting hollow-core and standard single-mode fibers with perfect mode-field size adaptation, Journal of Lightwave Technology. 42,6 (2023). https://doi.org/10.1109/JLT.2023.3329738.
35. Wang, C., et al., Ultralow-loss fusion splicing between negative curvature hollow-core fibers and conventional SMFs with a reverse-tapering method, Optics Express. 29,14 (2021). https://doi.org/10.1364/OE.432147.